CYCLIC ARC REGIMES IN SUBDUCTION ZONES AT CONSTANT PLATE MOTION, DUE TO FOLDING AT 660 KM DEPTH
INSIGHT FROM NUMERICAL MODELS - Gerbault M., Gibert G., Hassani R., Tric E.

GeoAzur TERRE · OCÉAN · ESPACE

Université Nice Sophia Antipolis

IRD Institut de recherche pour le développement

1– INTRODUCTION

Tomographic images show that a significant number of slabs stagnate in the transition zone around 660 km depth (e.g. Fukao et al. 2001). The interaction of the slab and the 660 km discontinuity may influence the temporal evolution of upper plate deformation and the migration of volcanic arcs over time is often related to changes in slab dip in the Southern and Central Andes, where three periods of 30–40 Ma of magmatic arc migration, are associated to variations in continental shortening and changing slab dip (Haschke et al. 2002; Ramos 2009).

Here we quantify the relationship between the kinematics of subduction, deformation in the overriding plate and the evolution of slab geometry. A 2-D finite element numerical code is used, and a first objective consists in benchmarking previously published analogue models (sections **2, 3**). Far-field plate velocities are applied and once the subducting plate reaches the 660 km discontinuity, modeled as a rigid base, we obtain different styles of subduction depending on the overriding plate velocity v_{op} (section **4**).

A kinematic phase diagram is deduced from a series of numerical tests, and we propose a velocity criterion from which the subduction zone evolves with time (section **5**). The geometry of the subduction is sensitive to the slab viscosity, and how the trench motion is sensitive to the strength of the overriding plate (see discussion and conclusion sections **6,7**).

2– NUMERICAL METHOD & ASSUMPTIONS

Appropriate boundary conditions for subduction dynamics are still debated, with two approaches :
- The first point of view from "mantle convection" considers the predominant role of the Stokes velocity of freely descending slabs (Christensen 1996; Schellart 2005; Goes et al. 2008).
- The other approach considers the solid-mechanics properties of tectonic plates, with plate strength, kinematics and interplate friction control arc stress regimes (Hassani et al. 1997; Gerbault et al. 2009; Yamato et al. 2009). We adopt this second viewpoint.

Our modeling approach is similar to that of Hassani et al., 1997, Bonnardot et al. 2008, or Buiter et al., 2001. Two visco-elastic lithospheric plates separated by a pre-defined fault overlie an inviscid asthenospheric mantle. Far field constant velocities are applied.

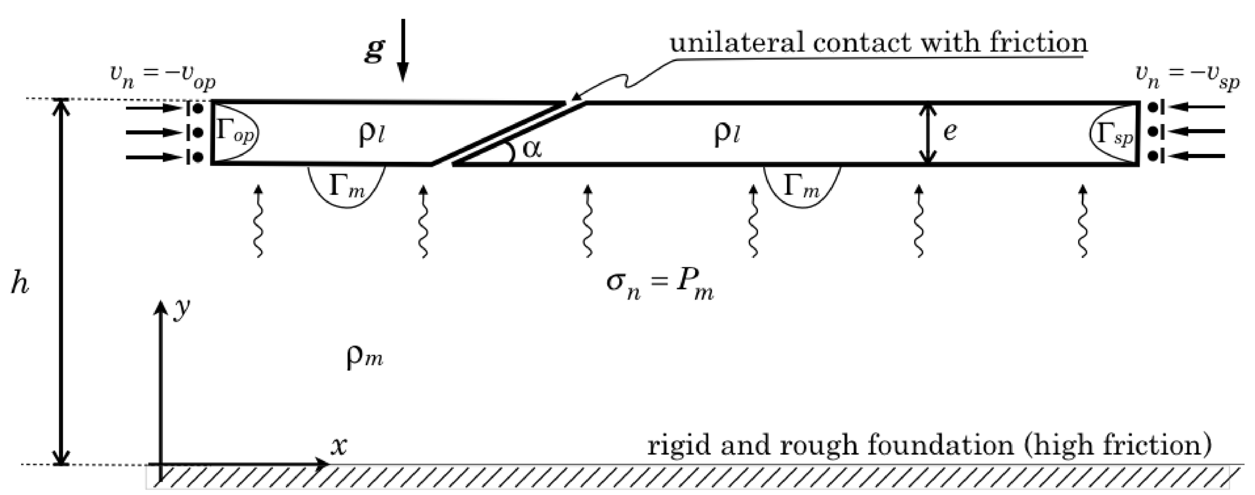

3- COMPARISON WITH ANALOG MODEL

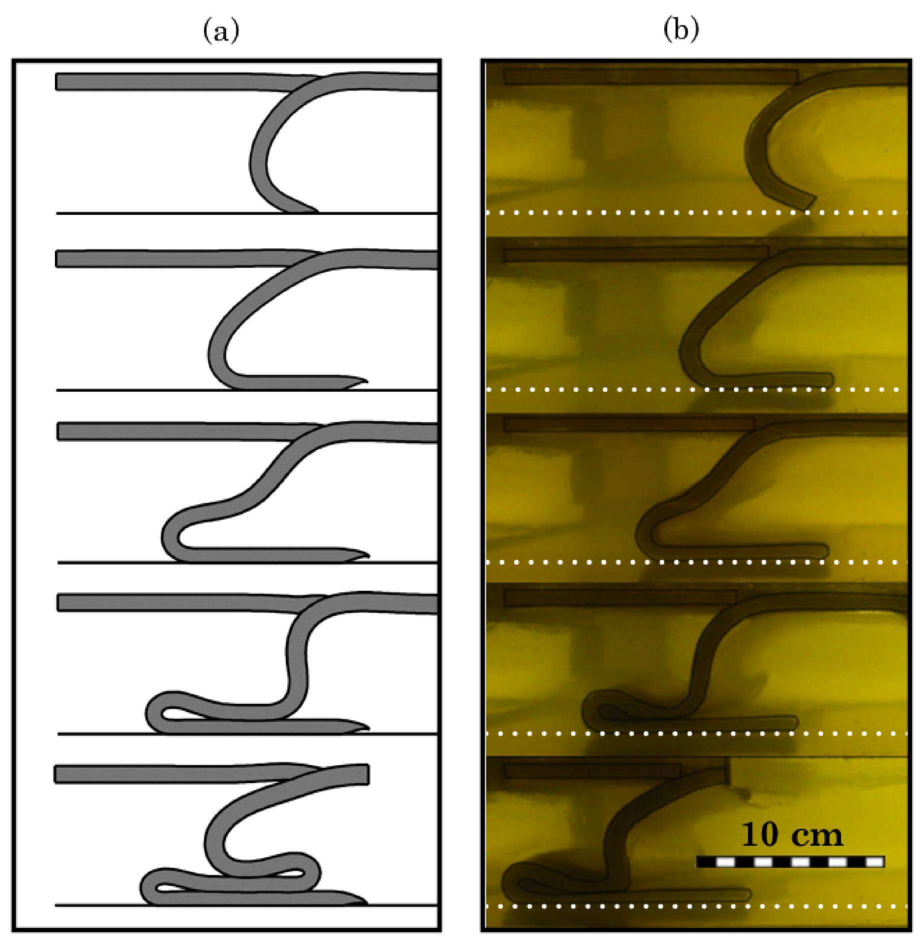

We first adopt the laboratory scale and assume similar dimensonless numbers as Guillaume et al. (2009).

Parameters	Values used in the laboratory scale model	Corresponding values at the natural scale
Plate thickness, e	13 mm	90 km
density contrast, $\Delta\rho = \rho_l - \rho_m$	$76\,\mathrm{kg\,m^{-3}}$	$76\,\mathrm{kg\,m^{-3}}$
Subducting plate velocity, v_{sp}	$1\,\mathrm{cm\,min^{-1}}$	$10\,\mathrm{cm\,a^{-1}}$
Simulation time, T	3300 s	38.8 Ma
Plate viscosity, η		
Subducting plate	5×10^5 Pa s	1.28×10^{24} Pa s
Overriding plate	3×10^5 Pa s	7.7×10^{23} Pa s
Young modulus, E	7000 Pa	4.85×10^{10} Pa
Poisson ratio, ν	0.25	0.25
Friction coefficients, μ		
Plate/plate	0.015	0.015
Plate/discontinuity	0.095	0.095
Viscosity ratio, η_m/η	0	0

The evolution is very similar in both models. There are two main differences:
- the trench position is almost unchanged in (a) while advancing in (b);
- the deep slab is anchored in (a), while it slips on the box bottom at the end of (b). Frictional coupling between plates and between the slab and the box bottom is modelled with a constant Coulomb friction in (a), but probably evolves during (b).

4– RESULTS : SUBDUCTION STYLES & MODES

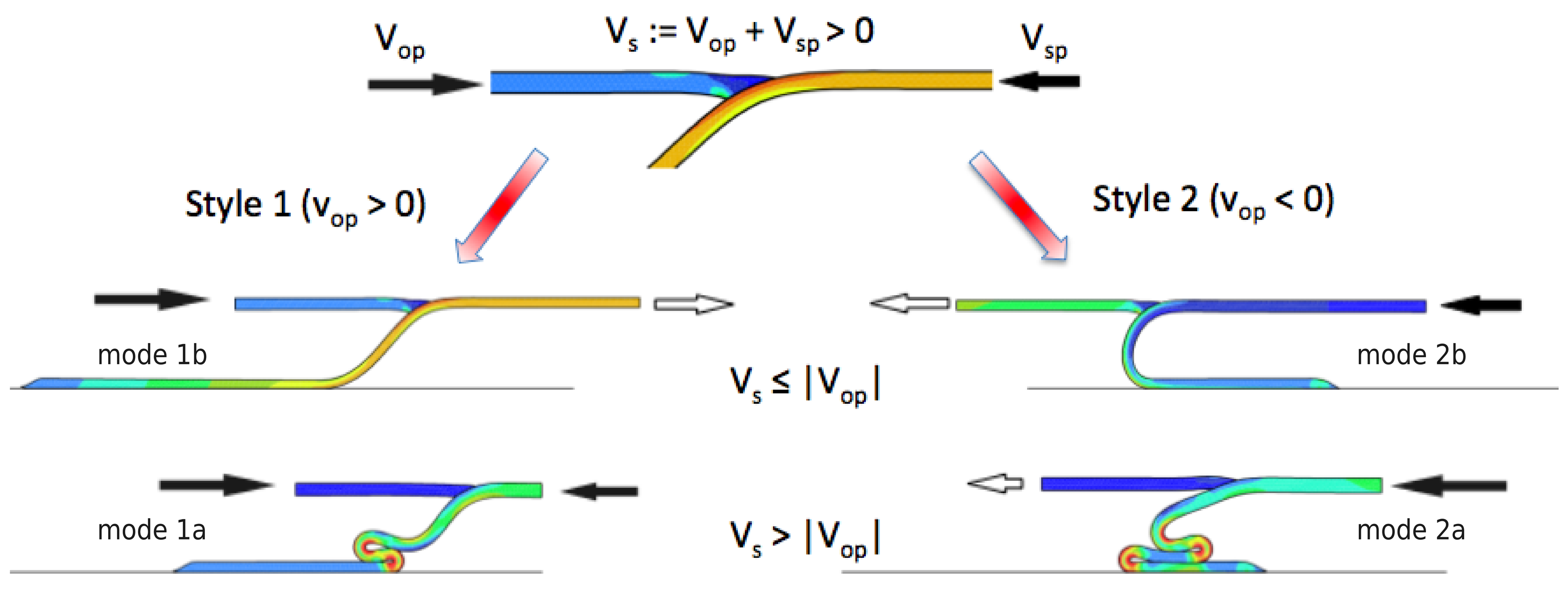

Parameters	Values
Plate thickness, e	90 km
Density contrast, $\Delta\rho = \rho_l - \rho_m$	$50\,\mathrm{kg\,m^{-3}}$
Subducting and overriding plate viscosities, η	10^{22} to 10^{26} Pa s
Young modulus, E	5×10^{10} Pa
Poisson ratio, ν	0.25
Friction coefficients, μ	
Plate/plate	0.01
Plate/discontinuity	0.2
Viscosity ratio, η_m/η	0
Subducting and overriding plate velocities, v_{op}, v_{sp}	-20 to $20\,\mathrm{cm\,a^{-1}}$

Four modes of subduction (2 for each style) occur depending on plates motions. Colours correspond to the second invariant of deviatoric strain, and arrows show far-field absolute plates velocities (black arrows are trenchward motion).

5 – RESULTS : CONDITIONS FOR CYCLICITY

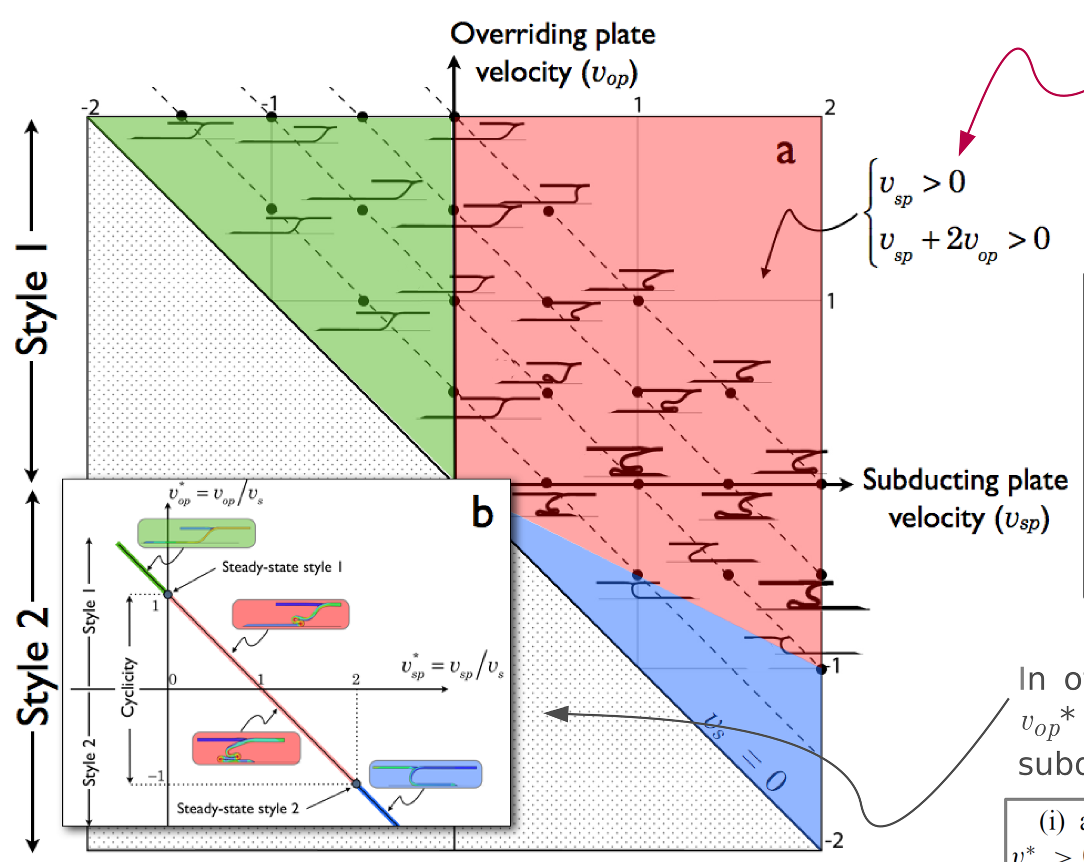

Cyclic behaviour takes place only when the absolute subduction velocity is greater than the upper plate velocity:

$v_{sp} + v_{op} > |v_{op}|$

$\begin{cases} v_{sp} > 0 \\ v_{sp} + 2v_{op} > 0 \end{cases}$

Style 1 : the slab lies forwards if $v_{op} > 0$ and

(i) mode 1a : the slab undergoes folding when $v_{sp} > 0$,
(ii) mode 1b : the slab can stretch (elongates) when $v_{sp} \leq 0$,

Style 2 : the slab lies backwards if $v_{op} \leq 0$ and

(i) mode 2a : the slab folds when $v_{sp} + 2v_{op} > 0$,
(ii) mode 2b : the slab can stretch when $v_{sp} + 2v_{op} \leq 0$.

In other dimensionless words (inset **b**), with $v_{op}^* = v_{op}/v_s$ (absolute velocity $v_s = v_{sp} + v_{op}$), subduction styles falls on the line $v_{sp}^* + v_{op}^* = 1$:

(i) a cyclic regime occurs when $-1 < v^*_{op} < 1$ (mode 1a if $v^*_{op} > 0$, otherwise mode 2a),
(ii) when $v^*_{op} > 1$ the slab stretches according to mode 1b,
(iii) when $v^*_{op} < -1$ the slab stretches according to mode 2b,
(iv) steady-state regimes occur for $|v^*_{op}| = 1$ (style 1 if $v^*_{op} = 1$, style 2 if $v^*_{op} = -1$).

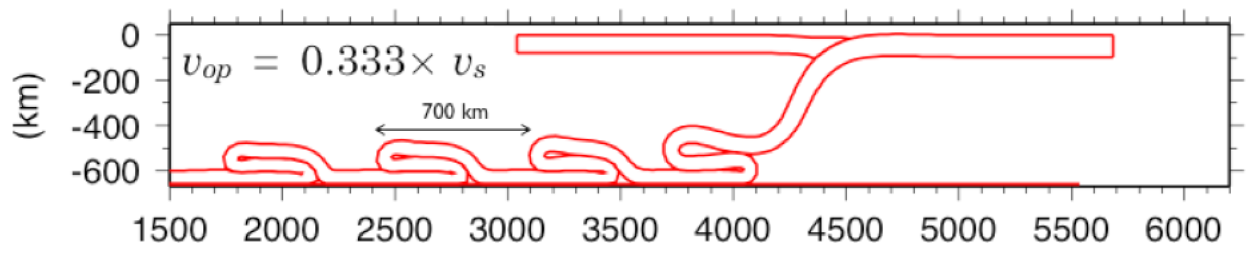

The periodicity of folds depends directly on the normalised velocity v_{op}^*.

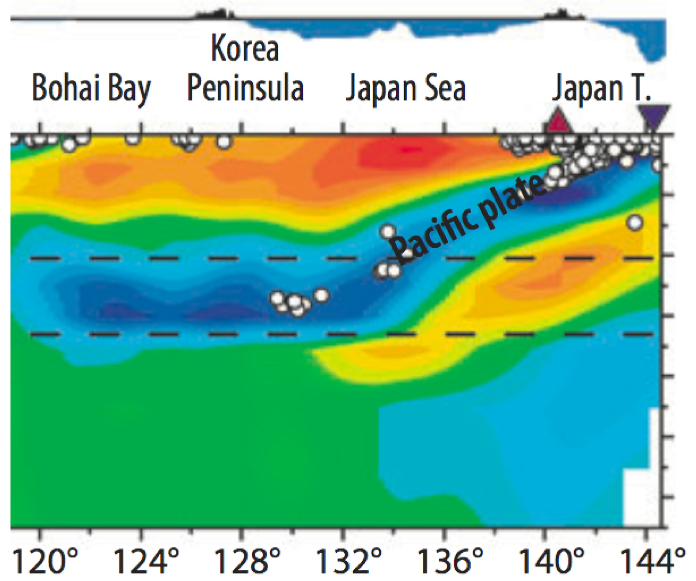

At latitudes 39–43°N (Fukao et al. 2009), the slab lying on the 660 km discontinuity appears to have a thickness twice that of the upper plate, which could be a result of slab folding and piling up (careful with uncertainities in spatial resolution and velocity in tomographic methods).
Kinematic estimates (DeMets et al. 2010) for the overriding Eurasian Plate are v_{op}= 20–24mm/yr, and Pacific Plate subduction at v_{sp}=63–69mm/yr. These values correspond to conditions for cyclic mode **1a.** Further investigation is required to link slab this with periodic deformation of the Eurasian overriding plate.

6 – RESULTS: OVERRIDING PLATE REGIME

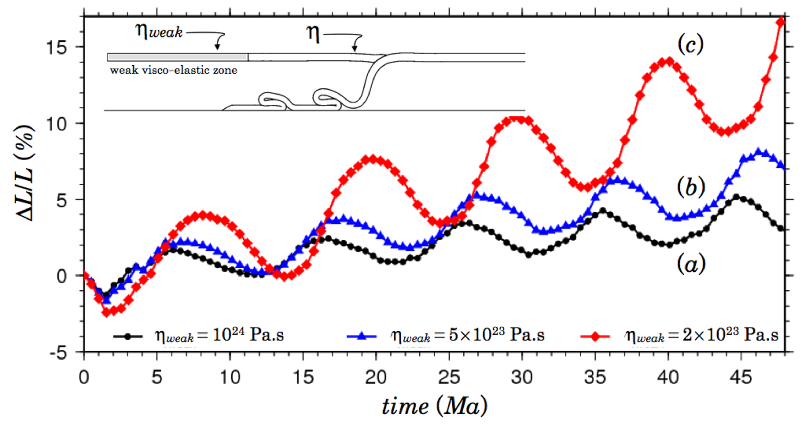

For our reference model in which plates viscosity is $\eta=10^{24}$ Pa.s, trench motion oscillates (black in figure). A weaker block inserted in the upper plate generates greater oscillation amplitudes (e.g. $\eta/5 = 2.10^{23}$ Pa s, in red). The periodicity of folding-induced oscillations increases with time, together with the periodicity of the folds at the base at 600 km depth, because the overriding plate thins and reduces its capacity to store stress.

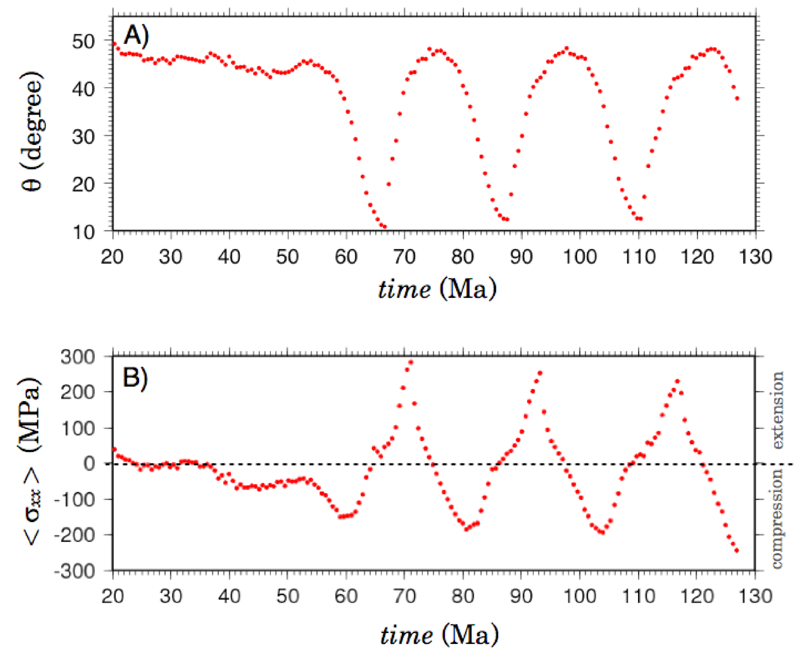

Along the Chilean margin, current plate velocities are v_{op}=4.3 cm/yr and v_{sp}=2.9 cm/yr (Nuvel-1A, v_s= v_{op}+ v_{sp}=7.2 cm/yr).
With $\eta=10^{24}$ Pa.s, our model produces cycles with a period ~22Ma and a shallow dip duration ~4.3Ma. Episodes of shallow slab (minimum dip angle=10°) may explain the observed gaps volcanic activity.
Discrepancy between model and observed slab dips (max modeled 48° against steepest observed 35°) can be explained by the absence of a viscous asthenospheric mantle (lack of viscous drag forces). On the other hand, the shallow present-day Nazca slab dip may not be at its maximum possible.

Seismic velocities (Fukao et al. 2009, Obayashi pers.com.) indicate variations in geometry of faster material above the 660 km domain.

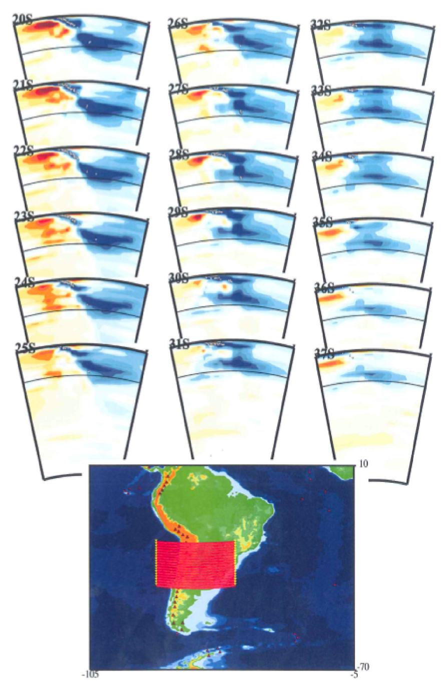

Compilation of magmatic-tectonic convergence parameters for the Andean margin in north and south Chile (details in Haschke et al., 2006).

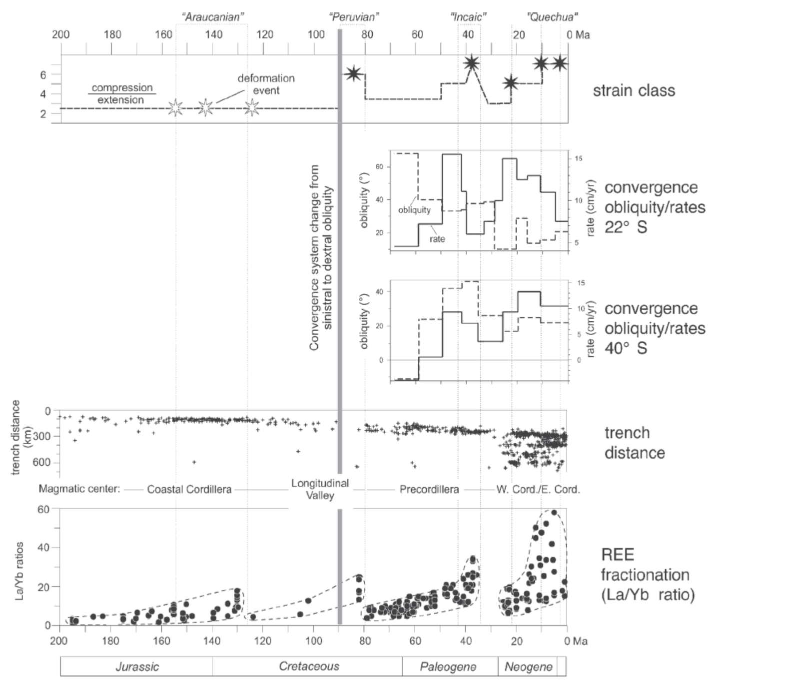

7– DISCUSSION

Because we applied far-field plate velocities, deformation of the homogeneous overriding plate thus links directly with velocities v_{op} and v_t (trench velocity). We observe:
- upper plate extension for modes **1b** and **2b** without cycles,
- upper plate shortening when the slab stackens (extension when it steepens) for modes **1a** and **2a**.

Modeling approaches of the first view point which account for slab/mantle mechanical interaction, still seldom account for the presence of the overriding plate, a free surface, and far-field imposed kinematic constraints. Although slab folding was also reproduced (Stegman et al., 2010), differences rise such as implications on trench motion.

The Stokes velocity of slabs competes with the motion imposed by tectonic boundary conditions. Goes et al. (2011) attributed the departure of observed slab velocities worldwide from modelled Stokes velocities (with freely subducting plates) to basal drag or other inner-mantle processes. While these processes are important, we make the point here that the kinematical constraints imposed by the Earth's surface are also of first-order importance.
We criticize modelling approaches assuming homogeneous slab viscosities of only 100 times greater that that of the mantle (generally < 2.10^{23} Pa s, e.g. Capitanio et al. 2010; Goes et al. 2008; Schellart 2009). A low-viscosity slab has little capacity in bending and stress storage (e.g. Ribe, 2010). Whereas low viscosities can be valid when approaching the 660 km zone, at the top surface it is important to consider higher viscosities. Experimental constraints on olivine around 900°C predict yield strengths of up to 1 GPa, and many studies have shown that tectonic plates sustain at least several hundreds of MPas (e.g. Ord & Hobbs 1989; Hassani et al. 1997; Gerbault et al., 2000).

Our models importantly neglect slab/mantle interaction. Modelling long-term subduction dynamics requires that temperature and compositionally dependent rheologies are accounted for in plates and in the mantle. Top surface processes as well as 3-D subduction effects are also factors that have been identified to play a first-order role as well... for future modelers!

Reference: Gibert et al.,2012, GJI v.189, 747–760.